Review

Mini and Micro Propulsion for Medical Swimmers

JianFeng [1] and Sung Kwon Cho [2],*

[1] Mechanical Engineering and Materials Science, Swanson School of Engineering, University of Pittsburgh, 616 Benedum Hall, 3700 O'Hara St., Pittsburgh, PA 15261, USA; E-Mail: jif17@pitt.edu

[2] Mechanical Engineering and Materials Science, Swanson School of Engineering, University of Pittsburgh, 538G Benedum Hall, 3700 O'Hara St., Pittsburgh, PA 15261, USA

* Author to whom correspondence should be addressed; E-Mail: skcho@pitt.edu; Tel.: +1-412-624-9798; Fax: +1-412-624-4846.

Abstract: Mini and micro robots, which can swim in an underwater environment, have drawn widespread research interests because of their potential applicability to the medical or biological fields, including delivery and transportation of bio-materials and drugs, bio-sensing, and bio-surgery. This paper reviews the recent ideas and developments of these types of self-propelling devices, ranging from the millimeter scale down to the micro and even the nano scale. Specifically, this review article makes an emphasis on various propulsion principles, including methods of utilizing smart actuators, external magnetic/electric/acoustic fields, bacteria, chemical reactions, *etc.* In addition, we compare the propelling speed range, directional control schemes, and advantages of the above principles.

Keywords: micro medical robot; microelectromechanical systems (MEMS); lab on a chip

1. Introduction

The classic movie, "Fantastic Voyage" (Figure 1) and the relatively recent movie "Inner Space", in which a miniaturized submarine and a crew navigate through blood streams to cure the abnormal areas in the human body, have inspired and stimulated many scientists and engineers to explore and realize such a medical microswimmer. Due to the advent of micro/nano fabrication technology and highly concerted inter/multi-disciplinary research activities, the realization of this kind of robot may not be

just science fiction anymore, but may possibly bring a revolution in medicine in the near future [1–3]. In developing such swimming medical robots, there are currently two major challenges: (1) lack of an efficient propelling and steering mechanism and (2) powering the robots. Thus far, numerous attempts have been made to tackle these challenges.

Generally speaking, there are two major physical mechanisms to generate a propulsion force in the small scale to overcome the drag force exerted by the surrounding liquid: "inertia propulsion" and "viscous propulsion" [4]. The inertia propulsion generates displacements of mass to exchange momentum between the swimming body and the surrounding fluid. The viscous propulsion uses viscous stresses with the surrounding fluid to generate a propulsion force. To classify these two propulsion mechanisms, the Reynolds number (*Re*), which stands for the ratio between the inertia force and the viscosity force, is commonly used. The Reynolds number is defined by *UL/v*, where *U* is the characteristic velocity (can be the propulsion speed or actuator speed), *L* the characteristic physical dimension (swimming body size or actuator size) and *v* the kinematic viscosity of the fluid. For the large *Re*, the inertia force is dominantly responsible for propulsion while for the small *Re* the viscous force is responsible. As the physical dimension critically affects *Re*, a suitable propulsion mechanism should be selected and used based on the size of the propulsion object or actuator.

This article reviews past and current research works on small-scale underwater propelling principles of the dimensions ranging from millimeters to nanometers. Here, *Re* is used to characterize propulsion principles. Propulsion over the size of millimeters may be too big to fit in the medical robots swimming inside of the human body. However, we include a brief review on it in the next section to show how the small-scale propulsion has evolved.

Figure 1. Snapshot in the movie (1966) "Fantastic Voyage" (miniaturized shuttle and crew navigate the human body).

2. Propulsion in Millimeter Scale

In the range of millimeter scales, a variety of smart actuators are commonly used to make the propulsion in a fluidic environment. Most of them are based on mimicking natural creatures as shown through the boxfish and tadpole. In addition, the fabrication is relatively easier than that of micro propulsion due to easy access to the large device scale with the well-developed macro scale manufacturing methods. Shape memory alloy (SMA) actuators are widely used to mimic the aquatic animal swimming. SMA is a solid smart material which uses electricity to store and exchange elastic energy. The advantage of SMA is that its structure is relatively simple and it can be actuated quietly

with electric current with a fast response. For example, an SMA manta ray robot was made in the size of 243 mm × 220 mm × 66 mm [5]. This manta could swim forward and turn with the maximum velocity of 57 mm/s (Re ~10^4). A similar idea was also used to build fins for a micro robot fish [6] and a jellyfish-like robot [7]. These types of swimming vehicles had the swimming speed in range of tens to hundred millimeters per second. The speed is mainly determined by the input signal frequency, voltage and duty ratio.

The ionic conducting polymerfilm (ICPF) is another type of actuator material that coverts electric energy into mechanical energy and works for mini robots in an aqueous medium. Guo *et al.* [8] used an ICPF actuator to make a robot fish (10 mm × 45 mm) and achieved a swimming motion with three degrees of freedom. By changing the input frequency, this robot could reach 5.21 mm/s (Re ~10^2) with the propulsion force of around 3.5 μN. Later, Guo *et al.* also developed another underwater vehicle by the ionic polymer metal composite (IPMC) [9]. The IPMC is usually durable, stable and has a fast response [10]. When the input voltage is applied to the IPMC membrane, the membrane bends because of ion motions associated with water molecules that are caused by the electric field. This IPMC fish had a similar size with the previous ICPF fish, and its swimming speed was 7 mm/s (Re ~10^2). The IPMC films were also used to connect styrene foams to make a snake-like robot [10] and a wireless undulatory tadpole robot [11].

The fin type propulsion was also achieved by piezoelectric piezoelectric actuators [12,13]. Deng *et al.* [13] made a boxfish-like mini robots (1 g) which used a four-bar structure to amplify the oscillation motion generated by the PZT bimorph actuators. The generated propulsion force by the sinusoidal signal was about 10% of the body weight. A boxfish type swimming minirobot can be driven by a thin bimorph giant magnetostrictive film (GMF) [14]. The primary and super harmonic resonances were used at a low frequency (<5 Hz) in a driving magnetic field to realize propulsion with the speed up to 4.67 mm/s (Re ~10^2).

For the above macroscale swimmers, the estimated Re numbers are over 10^2, which means the propulsion force is based on the inertia effects: The viscous effects are negligible. In the meantime, as opposed to the above active swimmers, there have been passive swimmers. For example, the PillCam (commercialized by Given Imaging, Inc., Yoqneam, Israel) of tens millimeters could travel through the gastrointestinal tract and take pictures [15]. However, this did not have a self-propelling system but its motion was generated by the muscle contraction of the human/animal body. It cannot be regarded as a robot with a controllable motion.

3. Propulsion in Micron and Nano Scale

When the dimension of swimming vehicles goes into the micro or nano scale, the propulsion principle is quite different from that of the larger scale. In addition, swimming in such a small scale faces a lot of challenges including spatial and temporal control of the swimming direction and speed [16]. In order to compare a variety of propulsion methods in micro/nano scale, the Reynolds number and propulsion speed are plotted in Figure 2. For reference, the data for some natural micro-organisms are added (Paramecium ~100 μm long, Human spermatozoon ~50 μm long and *Escherichia coli* ~3 μm long) [17,18]. Some of the fabricated micro devices could swim in the low Reynolds number region (even less than 10^{-5}), which are much smaller than the natural swimmers.
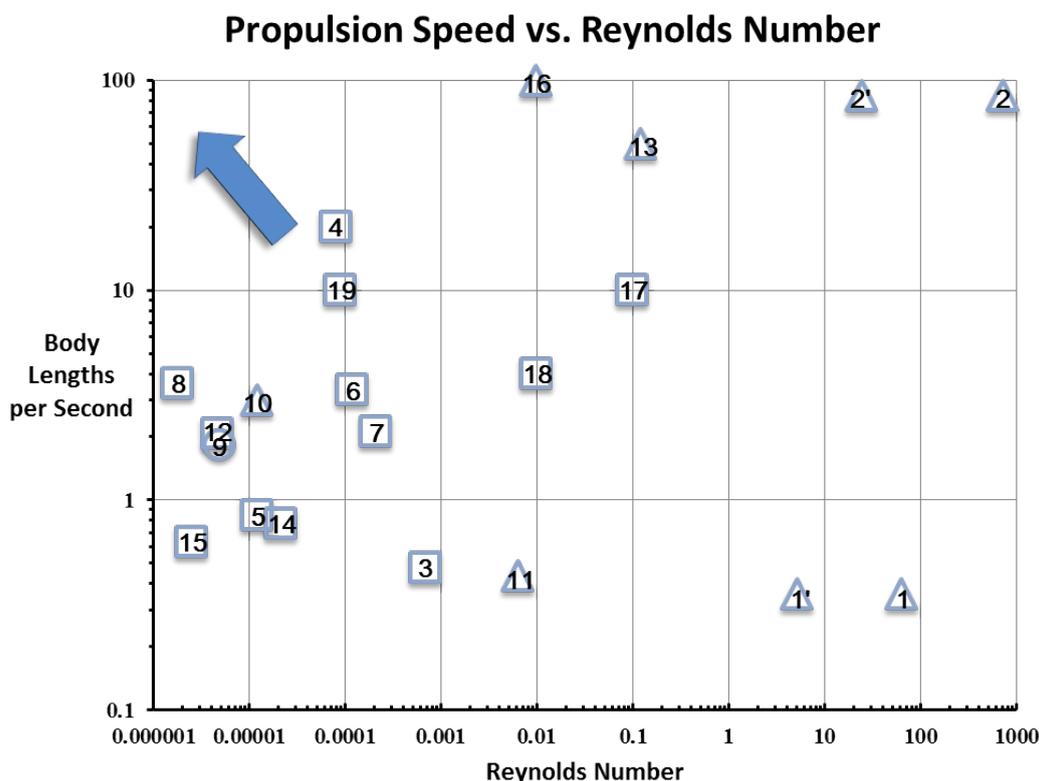
In general, however, the natural microorganisms have a relatively faster speed (~10 body lengths per second) than the artificial devices. Currently, almost all the developed propulsion devices do not generate a strong force high enough to propel against strong blood streams such as in aorta, but they can be operated in quiescent or mild flow regions. On the other hand, some swimmers that have a fast speed, for example, device 2 in Figure 2 cannot swim in the very low Reynolds number. The future research direction is expected to turn (*i.e.*, faster propulsion and smaller swimmer) toward the upper-left corner in the Figure 2 (indicated by the arrow).

For almost all of the swimming robots in the millimeter scale, the propulsion mechanisms are based on inertia propulsion. However, for the swimming robots in micro/nano scale, both inertia propulsion and viscous propulsion are possible, depending on the types of devices. From the authors' perspective, the developed propulsion mechanisms are classified as shown in Figure 2. The triangles in Figure 2 denote inertia-dominant propulsion; the squares denote viscous dominant propulsion; and the circles means the mechanisms are not clear. In Figure 2, the inertia propulsion methods are located in the large *Re* region while the viscous propulsion methods are in the low *Re* region. More specifically, the bubble type (putt-putt boat type) swimmers are using momentum transfer through the microstreaming formed by bubble oscillation [19,20]. The micro robots that harness natural organisms or use the artificial cilia/flagella (regardless of motion types, corkscrew motion, or flexible oar motion) generate propulsion via viscous stress interaction [17,18,21–26]. Among the chemical micro swimmers, even though there are still debates on the mechanism [27], some devices utilize the bubble recoiling method to make momentum transfer by inertia propulsion [28–31]. The electric and thermophoresis methods may be categorized as viscous propulsion, as the active Brownian motion method may [32–35].

3.1. Propulsion by Irreversible Strokes

If the Reynolds number is very low, the fluid motion can be easily reversed by simply reversing the stroke of the actuator. In other words, the motion created in one degree of freedom is always reciprocal (reversible), as stated in "the scallop theorem" [36]. Therefore, to generate propulsion in the low Reynolds number, making an irreversible motion is needed, for example a flexible oar motion and a corkscrew motion [36] that mimic that of many bacteria. There is a comparison between these two swimming modes showing that they have very comparable peak performance [37]. In addition to these two methods, there are other propulsion principles for micro robots that would work for the low Reynolds number, for example, the "Purcell's three-link swimmer" [36]. Becker *et al.* [38] made a detailed numerical study on this model. The results showed that this robot could swim in both directions along the straight line, however, the optimal three-link swimmer still had much less efficiency compared with the flexible oar motion or corkscrew motion. Najafi *et al.* [39] proposed another model with linearly linked three spheres for a micro robot that is operated based on the periodical internal motion. According to the numerical study, this swimmer could also work in the low Reynolds number range. Leoni *et al.* [40] first realized this model experimentally with optical tweezers and compared the experimental results with the numerical solution.

Figure 2. Propulsion speed and Reynolds number for artificial and natural micro swimmers. 1-acoustic scallop (*Re* is based on body speed and size) [19], 1′-acoustic scallop (*Re* is based on oscillating speed and amplitude), 2-oscillating micro bubble (*Re* is based on body speed and size) [20], 2′-oscillating micro bubble (*Re* is based on oscillating speed and amplitude), 3-artificial magnetic bacteria flagella [21], 4-artificial magnetic nanostructured propeller [22], 5-magnetically actuated colloidal [23], 6-magnetotactic bacteria propeller [24], 7-flagella-based propulsion [25], 8-active Brownian Janus [35], 9-self-motile colloidal [27], 10-catalytic nanomotor by bubble [28], 11-molecular motor [29], 12-striped metallic nanorod [32], 13-catalytic microtubular jet [30], 14-Pt-Au-Ppy motor with 1.05 μm radius cargo [33], 15-Au/Ni/Au/Pt-CNT motor with 4.3 μm diameter cargo [34], 16-Zinc microrockets [31], 17-paramecium [17], 18-human spermatozoon [17], and 19-*Escherichia coli* [18]. Note that the triangles denote inertia dominant propulsion, the squares denote viscous dominant propulsion, and the circles means the propulsion mechanisms cannot be clearly classified.
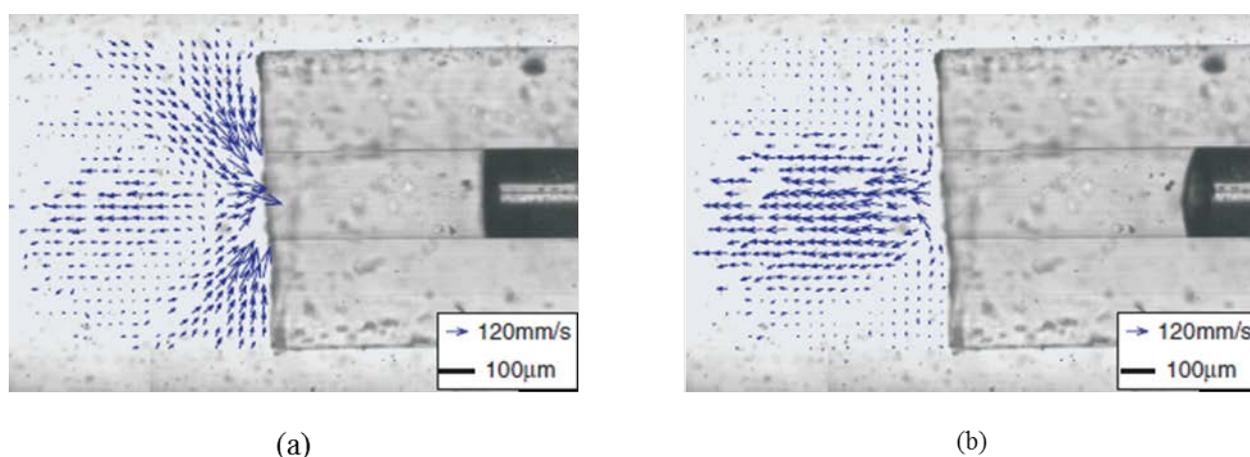

3.2. Propulsion by Bubbles

All the methods mentioned in the previous section are operated based on the irreversible motions. However, fast symmetric strokes still generate propulsion in the low Reynolds number. The key factor to get a better performance in this actuation is to increase the frequency of the motion to create a relatively large Reynolds number flow near the actuators, for example, using an actuator driven over several kHz [4]. Note that in this case the Reynolds number is based on the speed and size of the actuators, not the size and speed of body.

An oscillating bubble system allows us to easily and efficiently increase the frequency of the motion (speed of the induced flow). It is well known that when a gaseous bubble is periodically excited by an acoustic or temperature field, the bubble shrinks and expands as the oscillating wave of the pressure or temperature passes the bubble. Here, the high frequency oscillation generates a unidirectional, non-zero, time-averaged velocity component, which is called "micro streaming" [41]. The micro streaming flows have been applied to micropumps or micromixers [42,43].

Based on this idea, Dijkink *et al.* [19] built the "acoustic scallop" which is a millimeter scale acoustic "putt putt boat", using an air bubble (200–300 μm diameter and 2–4 mm long) trapped in a one-end open Teflon tube. By applying the acoustic field at the resonance frequency of the trapped bubble (1.55 kHz), which was generated by a piezoelectric transducer, the scallop was propelled by the bubble at the speed of about 1.35 mm/s. The theoretical calculation of the resonance frequency for the bubble in the tube was based on the spring-mass model developed by Chen *et al.* [44] and the previous experiments [45]. The propulsion force was calculated, based on the observation that the fluid patterns for the bubble shrinking and expansion processes were not symmetric, as shown in Figure 3a,b. A similar explanation was made by Jenkins [46,47], called "Machian Propulsion". If the Reynolds number UL/v is defined using the speed and size of the body, $Re \sim 5$, one may be understood that the inertia propulsion is not effective. However, if it is defined using the oscillation amplitude and speed of the bubble meniscus ($Re = 2R\omega_0 A/v$, where A is the bubble oscillation amplitude and ω_0 is angular frequency), $Re \sim 63$. As the latter Reynolds number of the generated flow is proportional to the operating frequency, it is high enough for the inertia to come into play to generate a net momentum transfer between the surrounding water and the "scallop" by oscillation of the bubble meniscus.

Figure 3. The flow field obtained from particle tracking velocimetry (PTV) at two phases of the acoustic cycle (**a**) phase 144° (intake flow); (**b**) phase 216° (outtake flow) [19].

(a)

(b)
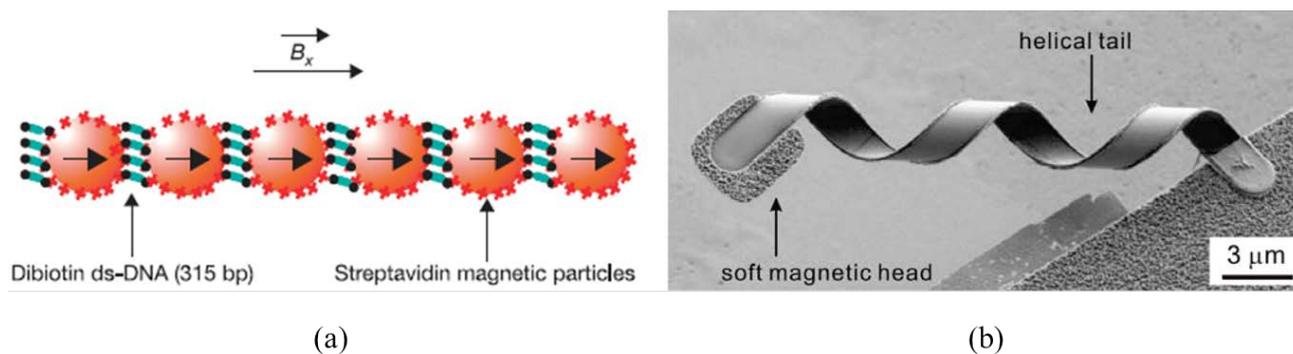
Later, Feng *et al.* [20] used a similar concept but in a much smaller scale by fabricating the micro scallop with a micron bubble (470 μm × 60 μm × 80 μm).The device is fabricated based on micro photolithography. This propulsion operated at the oscillation-based Reynolds number of around 700 and the body-based Reynolds number of about 24. A microswimmer with the capability of two dimensional steering was also developed later [48]. AC-electro wetting, other than the acoustic excitation, was also used to actuate oscillating bubbles (300 μm and 1.5 min diameter) to generate a steady streaming flow for propulsion [49]. The bubble oscillation was made by electrically changing

the contact angle of the bubbles [50]. In addition to the acoustic and electro wetting excitations, the thermal excitation could also be used for the similar propulsion [51] where the oscillation frequency was quite low (100 Hz).

3.3. Propulsion by Magnetic Field

The non-contact magnetic field actuation also draws a lot of attention to the micro robot propulsion with a possible application to *in vivo* drug delivery, nonsurgical exploration and navigation [52]. For instance, a spiral-type micro robot was designed by Ishiyama *et al.* [53], which mimicked the cilium propulsion of natural bacteria. The robot could even swim in high viscosity oil (500 mm^2/s) at a Reynolds number of about 10^{-7} and had a maximum velocity of 0.022 mm/s. Recently, the work has been extended to a smaller scale and lower Reynolds number. Similar to the "flexible oar motion" as mentioned above, Dreyfus *et al.* [54] developed a flexible artificial flagellum that was propelled by a propagating magnetic wave. The robot was made of red blood cells linearly chained by the magnetic colloids of 1-µm diameter and several DNA molecules of 107 nm in length, as shown in Figure 4a. When the homogenous and sinusoidal external magnetic fields were applied, a bending wave was generated in the filament, and the motion was non-reversible. Depending on the ratio between the tangential and perpendicular viscous coefficients, the filament swam towards the free end of the filament [55].

Figure 4. (**a**) Schematic of a DNA linked flexible magnetic filament [54]; (**b**) SEM image of ABF with diameter of 2.8 µm [21].

(a)   (b)

Williams *et al.* [26] also made this type of micro swimmer which was self-propelled. By the standard photolithography and dry etching process, polydimethylsiloxane (PDMS) filaments were made and attached to contractile cells. As the cells were selectively seeded on a single region of the filament, time-irreversible deformations were generated to produce the propulsion force. The best performance was achieved by the two-tailed swimmers with the velocity of 81 µm/s, about 8.3% body-lengths per second.
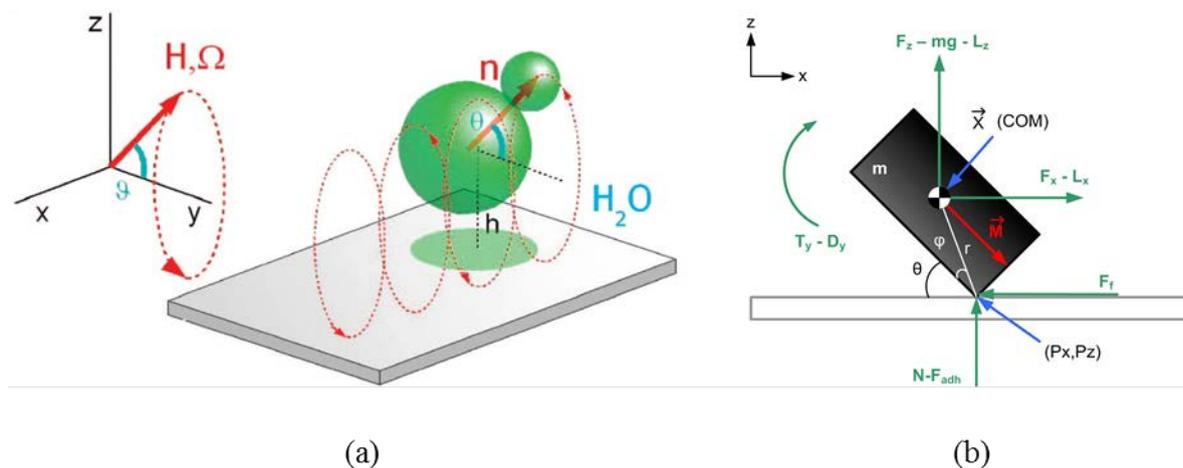
Another popular micro robot for the low Reynolds number is using the "corkscrew motion". A numerical model has been setup for this type of swimmer which gave the relation among the swimming velocity, efficiency, and external torque [56,57].

An artificial bacteria flagella (ABF) [58,59] was developed with a square soft-magnetic metal plate head and a helical tail using the anomalous scrolling process, as shown in Figure 4b [60].The ABF

with a 38-μm tail could swim forward and backward at the average speed of around 1.2μm/s by changing the rotation direction of the external magnetic field. The propulsion force of the 29-μm long ABF, which was estimated from the drag force of a single microsphere pushed by the ABF swimmer [58], was about 0.17 pN. Later, the authors quantitatively analyzed and mathematically modeled this 6-degree-of-freedom motion in comparison with the experiments. The model took into account the effect of the head, the magnetic field strength and the rotation frequency. The maximum velocity of ABF reached about 18 μm/s, and the propulsion force was calculated to be about 3.0 pN [21]. For similar swimming robots but several millimeters in size, more experiments in both water and glycerin were performed to compare the inertia and viscous forces [61]. Ghosh *et al.* [22] reduced the size of this magnetic propeller down to 200–300 nm wide and 1–2 μm long. The swimmer had a high propelling speed in water (~40 μm/s), which was much faster than the Brownian motion. Moreover, it showed a good steering ability. Based on a similar idea, Gao *et al.* [62] simplified the fabrication process by the template electro deposition protocol. The Au "head" and Ni "tail" were connected by a flexible sliver joint, which was dissolved in a peroxide solution. By changing the size of "head" and "tail", this device could move either forward or backward in a rotational magnetic field. Both head and tail could generate "cone surfaces" during rotation, and the amplitude was related with the size of the tail and head. The forces generated by both "head" and "tail" were proportional to the projection of the cone surface area in the direction of motion. As a result, the direction of motion could be controlled by changing the size of "head" and "tail".

In addition to the above propulsions, Tierno *et al.* [23] made another propulsion through non-reversible motions using the colloids doublet which had two spheres of 1.0 μm and 2.8 μm in diameter (Figure 5). The cDNA strands linked these two spheres. When the magnetic field was applied, the smaller sphere could rotate around the mass center in (x,z) plane and generate a viscous friction gradient in y direction by the boundary plate, as shown in Figure 5a. As a result, a motion in the x-direction was generated (up to 3.2 μm/s). Floyd *et al.* [63] demonstrated a micro-machined square shape magnetic robot (250 μm × 130 μm × 100 μm),which pushed a 116-μm diameter polystyrene bead in a water droplet under the magnetic control, as shown in Figure 5b.

Figure 5. (**a**) Schematic of the cDNA strands linked colloidal doublets motion in an external magnetic field [23]. (**b**) Schematic of the squared magnetic micro robot ($\overrightarrow{M}$ is magnetic vector) [63].

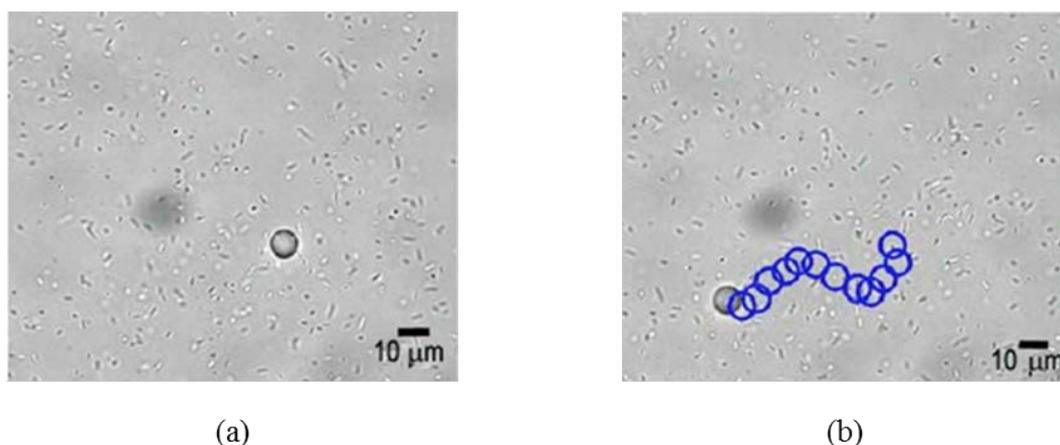(a)   (b)

3.4. Propulsion by Biological Mechanism

In addition to the artificial swimmers mimicking natural bacteria shown above, there have been research works directly harnessing the biological mechanism including natural bacteria and motor proteins.

Lee *et al.* demonstrated the assembly and transportation of magnetic nanoparticles by controlling the *Magnetospirillum magnetotacticum* [64]. Martel *et al.* [24] used the *Magnetospirillum gryphiswaldense* magnetotactic bacteria (MTB) to push a 3-μmdiameter bead and demonstrated propulsion at the average speed of 7.5 μm/s. As theMTB swims along the lines of geomagnetic field,thepropelling direction can be controlled. Behkam *et al.* [25] attached several *S. marcescens* bacteria to the 10-μm polystyrene sphere to make a swimming micro robot, as shown in Figure 6. The average speed of this robot could reach about 15 ± 6 μm/s. Interestingly, the stopping or resuming of the motion was controlled by copper ions or an ethylenediaminetetraacetic acid (EDTA) solution Hiratsuka *et al.* [65] made a micron size motor powered by bacteria that rotated at 1.5–2.6 rpm. The motor was pulled by gliding the bacterium Mycoplasma mobile along the track wall where the motor was docked. The binding between the track and the bacteria M. mobile was realized by the biotin-streptavidin interactions.

Figure 6. Phase-contrast optical image for the motion of a 10-μm diameter polystyrene bead propelled by *S. marcescens* bacteria at (**a**) *t* = 0 s and (**b**) *t* = 6 s [25].

(a)   (b)

Another biological propulsion was made by motor proteins that could move on a certain surface and be powered by the hydrolysis of adenosine triphosphate (ATP). Kinesin/microtubules are a typical structure to generate this type of motion. Tarhan *et al.* [66] improved the kinesin motion by separating the cargo loading and transporting mechanisms. By attaching the cargo to a nano-needle, the activity of kinesin did not be reduced, which enhanced to transport a variety of cargos. Fujimoto *et al.* [67] achieved the arranging of microtubules (kinesin or dynein) in an array in order to transport reactive molecules. More details could be seen in the reference [68].
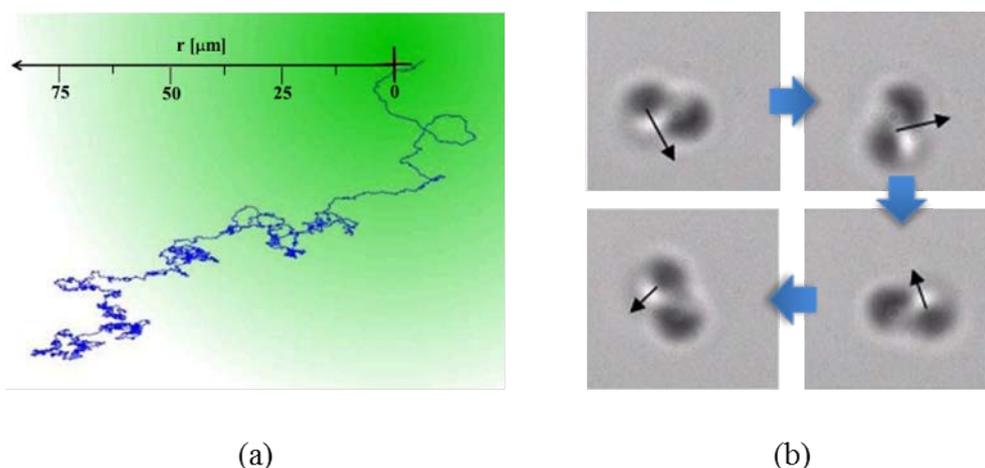
3.5. Propulsion by Active Brownian Motion and Self Thermophoresis

Unlike the Brownian motion in equilibrium, the active Brownian motion breaks the thermal equilibrium resulting in the particle motion or transportation in a controlled direction [69]. Volpe *et al.* [70]

made Janus particles with a gold coating on half of the silica spheres (radius 2.13 μm). When the incident light was absorbed by the golden coating part and, thus, the temperature exceeded the critical temperature, a local de-mixing could occur at the golden cap. This phenomenon would create a concentration difference that propels the particle: that is, an active Brownian motion occurred. The authors studied the swimming behavior of the Janus particles in the patterned surroundings and demonstrated the steering capability with the arranged obstacles. Buttinoni *et al.* [35] continued this study and showed a good direction control by changing the intensity of the green laser beam, which was used to generate the temperature difference in the Janus particle. The particle moved into the high light intensity area with the speed up to 0.7 μm/s. The trajectory of this particle is shown in Figure 7a.

Self-thermophoresis is a self-phoretic motion that is caused by the imbalanced osmotic effect on the solid-liquid interface. It could also be used for the micro particle propulsion. The propulsion speed for the self-thermophoresis is a function of temperature gradient on the particle surface [71]. As the Janus particle has a temperature difference by absorbing the laser light, a thermal slip flow would be generated. Jiang *et al.* [72] first measured this flow and controlled the particle motion by adjusting the laser power, as shown in Figure 7b.

Figure 7. (**a**) Trajectory of a self-propelled Janus particle by light gradient [35]; (**b**) rotational motion of a twin Janus particles by self-thermophoresis in defocused laser beam (time interval is 0.2 s) [72].

(a)   (b)

3.6. Propulsion by Chemical Reaction

Howse *et al.* [27] coated half of the polystyrene sphere (diameter 1.62 μm) with platinum. When this particle was placed in a hydrogen peroxide solution, it was propelled by breaking hydrogen peroxide into oxygen and water. In a short time period, the swimming was controlled by the hydrogen peroxide concentration at the speed of several μm/s. However, in a long time period, the propelling motion was random. This propulsion mechanism is not clearly understood yet as of today, though there have been two explanations introduced: the osmotic propulsion model and the bubble detachment propulsion model. An osmotic propulsion model [73] suggested that the swimming was caused by the non-equilibrium concentration of bath particles from the chemical reactions, and the osmotic pressure made the motion of fluid. Therefore, the swimming speed was mainly determined by the speeds of
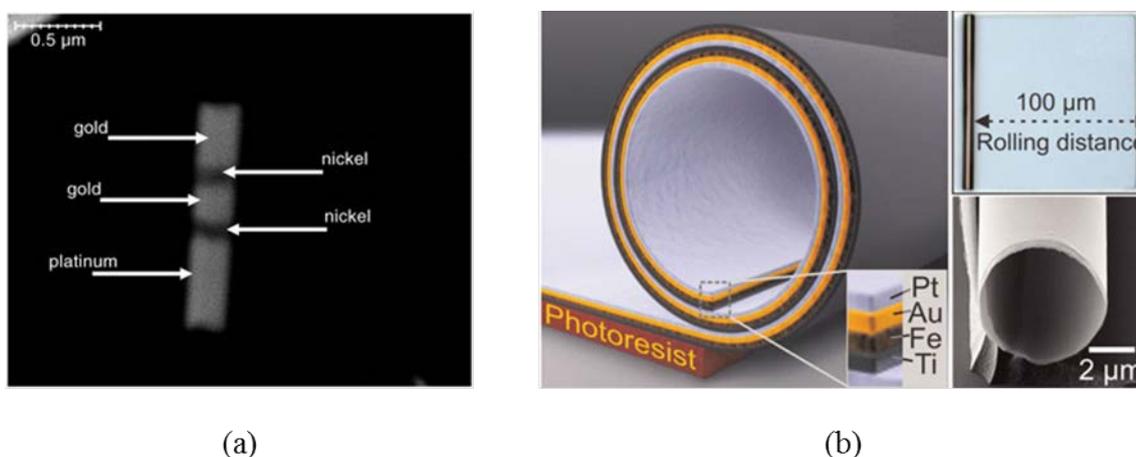
chemical reaction and particle diffusion. On the other hand, Gibbs *et al.* [28] suggested that this motion was caused by the growth and detachment of bubbles, which showed some agreement between theory and experiment.

Vicario *et al.* [29]used a molecular approach to demonstrate a nanoswimmer composed of the object (micro particle), the tether, and the catalyst motor. The swimmer used hydrogen peroxide to produce oxygen bubbles and converted chemical energy into mechanical energy. The recoiling of the bubbles could push the 80-μm-diameter silica particle at 35 μm/s in a CH$_3$CN solution and rotate it at 1.55×10^{-2} rad/s in glycerin.

Kline *et al.* [32] made a rod-like robot (1.5 μm long and 400 nm in diameter), which also used hydrogen peroxide for the propulsion fuel and platinum/gold for the catalyst. In addition, a nickel segment was used for the direction control, as shown in Figure 8a. When a magnetic field was applied, the rod could be aligned perpendicular to the magnetic field and moved in the direction of the platinum end. Paxton *et al.* [74] focused on the mechanism of the moving. They suggested that the movement was caused by the electro kinetic phenomenon. In other words, the ion flux formed in the electrical double layer at the solid-liquid interface could drag the molecules of solutions and cause the fluid motion. Based on this theory, Wang *et al.* [75] predicted the motion direction for different bimetallic nanorod configurations. The experimental results gave a consistent support to the electro kinetic mechanism.

Solovev *et al.* [30] developed a micro tubular jet using a multi-metallic film. The film had a platinum inner layer used for decomposing the hydrogen peroxide and a ferromagnetic layer for the magnetic direction control, as shown in Figure 8b. The robot had a larger opening to which the oxygen bubbles were driven and moved by the Laplace pressure difference. The hydro peroxide fuel was provided to the smaller opening end. As a result, a continuous jet flow and, thus, thrust was realized. The maximum speed of this cylinder was about 2 mm/s equal to around 50 body-lengths per second.

Figure 8. (**a**) Striped metallic nanorod 1.5 μm × 400 nm [32] and (**b**) Multi-metallic film for micro jet [30].

(a)　　　　　　　　　　　　　　　　(b)

Sundararajan *et al.* [33] showed acatalytic motor based on the hydrogenperoxide fuel by using electrophoresis (length <3.2 μm, diameter ~370nm) for thecolloidal cargo attachment and trasporation in a magnetic field. The magnetic field was used for the direction control. Burdick *et al.* [34] also

demonstrated the propulsion of the similar robots (~2 μm) in microchannel networks. They showed loading, transporting, and releasing of the spherical cargo. All of these were made by the magnetic force and viscous fluid drag.

Another chemical reaction propulsion is using polyaniline (PANI)/zinc in a strong acid solution to produce hydrogen bubbles [31]. Bipolar electrochemistry could be used for the metallic object swimming [76]. Through two redox reactions in the opposite ends of zinc dendrite, an electro osmotic flow was generated in the presence of electric field, and, thus, the dendrite was moved in the glass capillary.

Sumino *et al.* [77] studied the propulsion of an oil droplet. The motion mechanism is based on the difference of surface tension induced by non-equilibrium chemical conditions. By changing the boundary conditions, the random motion generated by the inverted convective flow inside of the oil droplet could be controlled and turned into a periodic regular motion or rotation.

In general, the advantages of the chemical micro swimmers are that they do not need power from the external system, such as magnetic field and acoustic field. Their dimensions could be easily reduced into nano scale. In particular, some of them show a high propulsion speed, even in such a nanoscale. However, the fuel, such as hydrogen peroxide solution or strong acids, may not be available *in vivo* environments and can be very harmful to the human and animal bodies. Moreover, to maintain this swimming, the chemical micro robots consume a certain chemical solution for the fuel, which gives many some challenging issues, including the limited lifetime.

4. Concluding Remarks and Challenges

In this paper, artificial swimmers are reviewed ranging from the millimeter scale down to the nano scale. The propulsion methods of the artificial swimmers are diverse including smart actuators, chemical reactions, bacteria mimicking, bacteria harness, bubble oscillation, *etc.* Many of them have shown exciting performances and promises with the ability of speed/direction control. However, each approach still has its own challenges to be addressed.

Most of the smarter actuators including SMA and ICPF are still operating in the millimeter scale and are tethered to an external power. For the bubble propulsion, it may be an issue to find the exact resonance frequency and efficiently transmit the acoustic field through the deep skin and bones. Resonating the bubbles is strongly influenced by the configurations of the bubbles and the surroundings. The magnetic propulsion shows a great swimming ability with six degree of freedom. However, it needs several external bulky coils that are orthogonally aligned to precisely control the magnetic field. The bacterial propulsion needs to maintain the controlled environment for the bacteria to survive, and the active Brownian motion is still difficult to exactly control the motion direction. For the chemical propulsion, chemical fuels that are not usually biologically compatible (are even harmful in some cases) are required to be provided and consumed.

In addition to the above challenges, there are common requirements. Powering of microswimmers is preferred to be wireless. The swimmers themselves and required fuels need to be biocompatible and even biodegradable, otherwise, they may be toxic to the human bodies during and after use. The microswimmers should be able to, on command, attach, transport, and release loads (biological materials) to finish the material transportation process. In addition, a good lifetime and stable working

properties are required. As all of these challenging issues are addressed, microswimming robots will get closer to the level of practical application.

Acknowledgements

Conflicts of Interest

The authors declare no conflict of interest.

References

1. Vince, G.; Wilson, C. The rise of the miniature medical robots. *New Sci.* **2009**, *204*, 50–53.
2. Sitti, M. Voyage of the microbots. *Nature* **2009**, *458*, 1121–1122.
3. Rubinstein, L. A Practical Nanorobot for Treatment of Various Medical Problems. In Proceedings of the 8th Foresight Conference on Molecular Nanotechnology, Bethesda, MD, USA, 2–5 November 2000.
4. Fukuda, T.; Kawamoto, A.; Arai, F.; Matsuura, H. Mechanism and Swimming Experiment of Micro Mobile Robot in Water. In Proceedings of the 1994 IEEE International Conference on Micro Electro Mechanical Systems, Oiso, Japan, 25–28 January 1994; pp. 273–278.
5. Wang, Z.; Wang, Y.; Li, J.; Hang, G. A Micro Biomimetic Manta Ray Robot Fish Actuated by SMA. In Proceedings of the 2009 IEEE International Conference on Robotics and Biomimetics, Guilin, China, 19–23 December 2009; pp. 1809–1813.
6. Wang, Z.; Hang, G.; Li, J.; Wang, Y.; Xiao, K. A micro-robot fish with embedded SMA wire actuated flexible biomimetic fin. *Sens. Actuators A* **2008**, *144*, 354–360.
7. Shi, L.; Guo, S.; Asaka, K. A Novel Jellyfish-Like Biomimetic Microrobot. In Proceedings of the 2010 IEEEI/ICME International Conference on Complex Medical Engineering, Gold Coast, Australia, 13–15 July 2010; pp. 277–281.
8. Guo, S.; Fukuda, T.; Asaka, K. A new type of fish-like underwater microrobot. *IEEE/ASME Trans. Mechatron.* **2003**, *8*, 136–141.
9. Guo, S.; Ge, Y. Underwater Swimming Micro Robot Using IPMC Actuator. In Proceedings of the 2006 IEEE International Conference on Mechatronics and Automation, Luoyang, China, 25–28 June 2006; pp. 249–254.
10. Kamamichi, N.; Yamakita, M.; Asaka, K.; Luo, Z.-W. A Snake-Like Swimming Robot Using IPMC Actuator/Sensor. In Proceedings of the 2006 IEEE International Conference on Robotics and Automation, Orlando, FL, USA, 15–19 May 2006; pp. 1812–1817.
11. Kim, B.; Kim, D.-H.; Jung, J.; Park, J.-O. A biomimetic undulatory tadpole robot using ionic polymer-metal composite actuators. *Smart Mater. Struct.* **2005**, *14*, 1579–1585.
12. Ming, A.; Park, S.; Nagata, Y.; Shimojo, M. Development of Underwater Robots Using Piezoelectric Fiber Composite. In Proceedings of the 2009 IEEE International Conference on Robotics and Automation, Kobe, Japan, 12–17 May, 2009; pp. 3821–3826.

13. Deng, X.; Avadhanula, S. Biomimetic Micro Underwater Vehicle with Oscillating Fin Propulsion: System Design and Force Measurement. In Proceedings of the 2005 IEEE International Conference on Robotics and Automation, Barcelona, Spain, 18–22 April 2005; pp. 3312–3317.

14. Liu, W.; Jia, X.; Wang, F.; Jia, Z. An in-pipe wireless swimming microrobot driven by giant magnetostrictive thin film. *Sens. Actuators A* **2010**, *160*, 101–108.

15. Toennies, J.L.; Tortora, G.; Simi, M.; Valdastri, P.; Webster, R.J. Swallowable medical devices for diagnosis and surgery: The state of the art. *J. Mech. Eng. Sci.* **2010**, *224*, 1397–1414.

16. Wang, J.; Manesh, K.M. Motion control at the nanoscale. *Small* **2009**, *6*, 338–345.

17. Lauga, E.; Powers, T.R. The hydrodynamics of swimming microorganisms. *Rep. Prog. Phys.* **2009**, *72*, 096601; doi:10.1088/0034-4885/72/9/096601.

18. Brennen, C.; Winet, H. Fluid mechanics of propulsion by cilia and flagella. *Ann. Rev. Fluid Mech.* **1977**, *9*, 339–398.

19. Dijkink, R.J.; Dennen, van der Dennen, J.P.; Ohl, C.D.; Prosperetti, A. The "acoustic scallop": A bubble-powered actuator. *J. Micromech. Microeng.* **2006**, *16*, 1653–1659.

20. Feng, J.; Cho, S.K. Micro Propulsion in Liquid by Oscillating Bubbles. In Proceedings of the 2013 IEEE 26th International Conference on Micro Electro Mechanical Systems, Taipei, Taiwan, 20–24 January 2013; pp. 63–66.

21. Zhang, L.; Abbott, J.J.; Dong, L.; Peyer, K.E.; Kratochvil, B.E.; Zhang, H.; Bergeles, C.; Nelson, B.J. Characterizing the swimming properties of artificial bacterial flagella. *Nano Lett.* **2009**, *9*, 3663–3667.

22. Ghosh, A.; Fischer, P. Controlled propulsion of artificial magnetic nanostructured propellers. *Nano Lett.* **2009**, *9*, 2243–2245.

23. Tierno, P.; Golestanian, R.; Pagonabarraga, I.; Sagués, F. Magnetically actuated colloidal microswimmers. *J. Phys. Chem. B* **2008**, *112*, 16525–16528.

24. Martel, S.; Tremblay, C.C.; Ngakeng, S.; Langlois, G. Controlled manipulation and actuation of micro-objects with magnetotactic bacteria. *Appl. Phys. Lett.* **2006**, *89*, 233904; doi:10.1063/1.2402221.

25. Behkam, B.; Sitti, M. Bacterial flagella-based propulsion and on/off motion control of microscale objects. *Appl. Phys. Lett.* **2007**, *90*, 023902; doi:10.1063/1.2431454.

26. Williams, B.J.; Anand, S.V.; Rajagopalan, J.; Saif, M.T.A. A self-propelled biohybrid swimmer at low Reynolds number. *Nat. Commun.* **2014**, *5*, 3081; doi:10.1038/ncomms4081.

27. Howse, J.R.; Jones, R.A.L.; Ryan, A.J.; Gough, T.; Vafabakhsh, R.; Golestanian, R. Self-motile colloidal particles: From directed propulsion to random walk. *Phys. Rev. Lett.* **2007**, *99*, 048102; doi:10.1103/PhysRevLett.99.048102.

28. Gibbs, J.G.; Zhao, Y.-P. Autonomously motile catalytic nanomotors by bubble propulsion. *Appl. Phys. Lett.* **2009**, *94*, 163104; doi:10.1063/1.3122346.

29. Vicario, J.; Eelkema, R.; Browne, W.R.; Meetsma, A.; Crois, R.M.L.; Feringa, B.L. Catalytic molecular motors: Fuelling autonomous movement by a surface bound synthetic manganese catalase. *Chem. Commun.* **2005**, 3936–3938.

30. Solovev, A.A.; Mei, Y.; Ureña, E.B.; Huang, G.; Schmidt, O.G. Catalytic microtubular jet engines self-propelled by accumulated gas bubbles. *Small* **2009**, *5*, 1688–1692.

31. Gao, W.; Uygun, A.; Wang, J. Hydrogen-bubble-propelled zinc-based microrockets in strongly acidic media. *J. Am. Chem. Soc.* **2012**, *134*, 897–900.

32. Kline, T.R.; Paxton, W.F.; Mallouk, T.E.; Sen, A. Catalytic nanomotors: Remote-controlled autonomous movement of striped metallic nanorods. *Angew. Chem. Int. Ed.* **2005**, *44*, 744–746.

33. Sundararajan, S.; Lammert, P.E.; Zudans, A.W.; Crespi, V.H.; Sen, A. Catalytic motors for transport of colloidal cargo. *Nano Lett.* **2008**, *8*, 1272–1276.

34. Burdick, J.; Laocharoensuk, R.; Wheat, P.M.; Posner, J.D.; Wang, J. Synthetic nanomotors in microchannel networks: Directional microchip motion and controlled manipulation of cargo. *J. Am. Chem. Soc.* **2008**, *130*, 8164–8165.

35. Buttinoni, I.; Volpe, G.; Kümmel, F.; Volpe, G.; Bechinger, C. Active Brownian motion tunable by light. *J. Phys. Condens. Matter* **2012**, *24*, 284129; doi:10.1088/0953-8984/24/28/284129.

36. Purcell, E.M. Life at low Reynolds number. *Am. J. Phys.* **1977**, *45*, 3–11.

37. Abbott, J.J.; Peyer, K.E.; Lagomarsino, M.C.; Zhang, L.; Dong, L.; Kaliakatsos, I.K.; Nelson, B.J. How should microrobots swim? *Int. J. Robot. Res.* **2009**, *28*, 1434–1447.

38. Becker, L.E.; Koehler, S.A.; Stone, H.A. On self-propulsion of micro-machines at low Reynolds number: Purcell's three-link swimmer. *J. Fluid Mech.* **2003**, *490*, 15–35.

39. Najafi, A.; Golestanian, R. A simplest swimmer at low Reynolds number: Three linked spheres. *Phys. Rev. E* **2004**, *69*, 062901; doi:10.1103/PhysRevE.69.062901.

40. Leoni, M.; Kotar, J.; Bassetti, B.; Cicuta, P.; Lagomarsino, M.C. A basic swimmer at low Reynolds number. *Soft Matter* **2009**, *5*, 472–476.

41. Plesset, M.S.; Prosperetti, A. Bubble dynamics and cavitation. *Ann. Rev. Fluid Mech.* **1977**, *9*, 145–185.

42. Ahmed, D.; Mao, X.; Shi, J.; Juluri, B.K.; Huang, T.J. A millisecond micromixer via single-bubble-based acoustic streaming. *Lab Chip* **2009**, *9*, 2738–2741.

43. Tsai, J.-H.; Lin, L. Active microfluidic mixer and gas bubble filter driven by thermal bubble micropump. *Sens. Actuators A* **2002**, *97–98*, 665–671.

44. Chen, X.M.; Prosperetti, A. Thermal processes in the oscillations of gas bubbles in tubes. *J. Acoust. Soc. Am.* **1998**, *104*, 1389–1398.

45. Geng, X.; Yuan, H.; Oğuz, H.N.; Prosperetti, A. The oscillation of gas bubbles in tubes: Experimental results. *J. Acoust. Soc. Am.* **1999**, *106*, 674–681.

46. Jenkins, A. An elementary treatment of the reverse sprinkler. *Am. J. Phys.* **2004**, *72*, 1276–1282.

47. Jenkins, A. Sprinkler head revisited: Momentum, forces, and flows in machian propulsion. *Eur. J. Phys.* **2011**, *32*, 1213–1226.

48. Feng, J.; Cho, S.K. Two-Dimensionally Steering Microswimmer Propelled by Oscillating Bubbles. In Proceedings of the 2014 IEEE 27th International Conference on Micro Electro Mechanical Systems, San Francisco, CA, USA, 26–30 January 2014.

49. Ryu, K.; Zueger, J.; Chung, S.K.; Cho, S.K. Underwater Propulsion Using AC-Electrowetting-Actuated Oscillating Bubbles for Swimming Robots. In Proceedings of the 2010 IEEE 23rd International Conference on Micro Electro Mechanical Systems, Wanchai, Hong Kong, 24–28 January 2010; pp. 160–163.

50. Zhao, Y.; Cho, S.K. Micro air bubble manipulation by electrowetting on dielectric (EWOD): Transporting, splitting, merging and eliminating of bubbles. *Lab Chip.* **2007**, *7*, 273–280.

51. Qiao, L.; Luo, C. Propulsion of a microsubmarine using a thermally oscillatory approach. *J. Micromech. Microeng.* **2013**, *23*, 105011; doi:10.1088/0960-1317/23/10/105011.

52. Gillies, G.T.; Ritter, R.C.; Broaddus, W.C.; Grady, M.S.; Howard, M.A.I.; McNeil, R.G. Magnetic manipulation instrumentation for medical physics research. *Rev. Sci. Instrum.* **1994**, *65*, 533–562.

53. Ishiyama, K.; Arai, K.I.; Sendoh, M.; Yamazaki, A. Spiral-Type Micro-Machine for Medical Applications. In Proceedings of the 2000 International Symposium on Micromechatronics and Human Science, Nagoya, Japan, 22–25 October 2000; pp. 65–69.

54. Dreyfus, R.; Baudry, J.; Roper, M.L.; Fermigier, M.; Stone, H.A.; Bibette, J. Microscopic artificial swimmers. *Nature* **2005**, *437*, 862–865.

55. Cox, R.G. Motion of long slender bodies in a viscous fluid. Part I. General theory. *J. Fluid Mech.* **1970**, *44*, 791–810.

56. Purcell, E.M. The efficiency of propulsion by a rotating flagellum. *Proc. Natl. Acad. Sci. USA* **1997**, *94*, 11307–11311.

57. Chattopadhyay, S.; Moldovan, R.; Yeung, C.; Wu, X.L. Swimming efficiency of bacterium Escherichia coli. *Proc. Natl. Acad. Sci. USA* **2006**, *103*, 13712–13717.

58. Zhang, L.; Abbott, J.J.; Dong, L.; Kratochvil, B.E.; Bell, D.; Nelson, B.J. Artificial bacterial flagella: Fabrication and magnetic control. *Appl. Phys. Lett.* **2009**, *94*, 064107; doi:10.1063/1.3079655.

59. Bell, D.J.; Leutenegger, S.; Hammar, K.M.; Dong, L.X.; Nelson, B.J. Flagella-Like Propulsion for Microrobots Using a Nanocoil and a Rotating Electromagnetic Field. In Proceedings of the 2007 IEEE International Conference on Robotics and Automation, Roma, Italy, 10–14 April 2007; pp. 1128–1133.

60. Zhang, L.; Ruh, E.; Grützmacher, D. Anomalous coiling of SiGe/Si and SiGe/Si/Cr helical nanobelts. *Nano Lett.* **2006**, *6*, 1311–1317.

61. Temel, F.Z.; Yesilyurt, S. Magnetically Actuated Micro Swimming of Bio-Inspired Robots in Mini Channels. In Proceedings of the 2011 IEEE Intemational Conference on Mechatronics, Istanbul, Turkey, 13–15 April 2011; pp. 342–347.

62. Gao, W.; Sattayasamitsathit, S.; Manesh, K.M.; Weihs, D.; Wang, J. Magnetically powered flexible metal nanowire motors. *J. Am. Chem. Soc.* **2010**, *132*, 14403–14405.

63. Floyd, S.; Pawashe, C.; Sitti, M. An Untethered Magnetically Actuated Micro-Robot Capable of Motion on Arbitrary Surfaces. In Proceedings of the 2008 IEEE International Conference on Robotics and Automation, Pasadena, CA, USA, 19–23 May 2008; pp. 419–424.

64. Lee, H.; Purdon, A.M.; Chu, V.; Westervelt, R.M. Controlled assembly of magnetic nanoparticles from magnetotactic bacteria using microelectromagnets arrays. *Nano Lett.* **2004**, *4*, 995–998.

65. Hiratsuka, Y.; Miyata, M.; Tada, T.; Uyeda, T.Q.P. A microrotary motor powered by bacteria. *PNAS* **2006**, *103*, 13618–13623.

66. Tarhan, M.C.; Yokokawa, R.; Bottier, C.; Collard, D.; Fujita, H. A nano-needle/microtubule composite gliding on a kinesin-coated surface for target molecule transport. *Lab Chip.* **2010**, *10*, 86–91.

67. Fujimoto, K.; Kitamura, M.; Yokokawa, M.; Kanno, I.; Kotera, H.; Yokokawa, R. Colocalization of quantum dots by reactive molecules carried by motor proteins on polarized microtubule arrays. *ACS Nano* **2013**, *7*, 447–455.

68. Vogel, V.; Hess, H. Nanoshuttles: Harnessing Motor Proteins to Transport Cargo in Synthetic Environments. In *Controlled Nanoscale Motion*; Linke, H.; Månsson, A., Eds.; Springer: Heidelberg, Germany, 2007; pp. 367-383.

69. Hanggi, P.; Marchesoni, F. Artificial Brownian motors: Controlling transport on the nanoscale. *Rev. Mod. Phys.* **2009**, *81*, 387–442.

70. Volpe, G.; Buttinoni, I.; Vogt, D.; Kümmerer, H.-J.; Bechinger, C. Microswimmers in patterned environments. *Soft Matter* **2011**, *7*, 8810–8815.

71. Golestanian, R.; Liverpool, T.B.; Ajdari, A. Designing phoretic micro- and nano-swimmers. *New J. Phys.* **2007**, *9*, 126; doi:10.1088/1367-2630/9/5/126.

72. Jiang, H.-R.; Yoshinaga, N.; Sano, M. Active motion of a Janus particle by self-thermophoresis in a defocused laser beam. *Phys. Rev. Lett.* **2010**, *105*, 268302; doi:10.1103/PhysRevLett.105.268302.

73. Córdova-Figueroa, U.M.; Brady, J.F. Osmotic propulsion: The osmotic motor. *Phys. Rev. Lett.* **2008**, *100*, 158303; doi :10.1103/PhysRevLett.100.158303.

74. Paxton, W.F.; Baker, P.T.; Kline, T.R.; Wang, Y.; Mallouk, T.E.; Sen, A. Catalytically induced electrokinetics for motors and micropumps. *J. Am. Chem. Soc.* **2006**, 14881–14888.

75. Wang, Y.; Hernandez, R.M.; Bartlett, D.J., Jr.; Bingham, J.M.; Kline, T.R.; Sen, A.; Mallouk, T.E. Bipolar electrochemical mechanism for the propulsion of catalytic nanomotors in hydrogen peroxide solutions. *Langmuir* **2006**, *22*, 10451–10456.

76. Loget, G.; Kuhn, A. Propulsion of microobjects by dynamic bipolar self-regeneration. *J. Am. Chem. Soc.* **2010**, *132*, 15918–15919.

77. Sumino, Y.; Magome, N.; Hamada, T.; Yoshikawa, K. Self-running droplet: Emergence of regular motion from nonequilibrium noise. *Phys. Rev. Lett.* **2005**, *94*, 068301; doi:10.1103/PhysRevLett.94.068301.